

# High quality sub-monolayer, monolayer, and bilayer graphene on Ru(0001)\*

Xu Wen-Yan(徐文焱), Huang Li(黄立), Que Yan-De(阙炎德), Li En(李恩), Zhang Hai-Gang(张海刚), Lin Xiao(林晓)<sup>†</sup>, Wang Ye-Liang(王业亮)<sup>‡</sup>, Du Shi-Xuan(杜世萱), and Gao Hong-Jun(高鸿钧)<sup>§</sup>

*Institute of Physics, Chinese Academy of Sciences, Beijing 100190, China*

*University of Chinese Academy of Sciences, Beijing 100049, China*

(Received 29 April 2014; revised manuscript received 6 May 2014; published online 16 July 2014)

High quality sub-monolayer, monolayer, and bilayer graphene were grown on Ru(0001). For the sub-monolayer graphene, the size of graphene islands with zigzag edges can be controlled by the dose of ethylene exposure. By increasing the dose of ethylene to 100 Langmuir at a high substrate temperature (800 °C), high quality single-crystalline monolayer graphene was synthesized on Ru(0001). High quality bilayer graphene was formed by further increasing the dose of ethylene while reducing the cooling rate to 5 °C/min. Raman spectroscopy revealed the vibrational states of graphene, G and 2D peaks appeared only in the bilayer graphene, which demonstrates that it behaves as the intrinsic graphene. Our present work affords methods to produce high quality sub-monolayer, monolayer, and bilayer graphene, both for basic research and applications.

**Keywords:** graphene, Ru(0001), scanning tunneling microscopy

**PACS:** 81.05.ue, 68.65.Pq, 87.64.Dz

**DOI:** 10.1088/1674-1056/23/9/098101

## 1. Introduction

The discovery of graphene by Novoselov *et al.* opened new avenues for fundamental physical study and potential electronics applications.<sup>[1]</sup> This sp<sup>2</sup>-bonded two-dimensional carbon network exhibits many fascinating properties, which are related to the linear dispersion of its  $\pi$  and  $\pi^*$  bands,<sup>[2]</sup> huge carrier mobility,<sup>[3–5]</sup> ballistic transport at room temperature,<sup>[6]</sup> and half-integer quantum Hall effect.<sup>[7,8]</sup> These properties could lead to many promising applications in future graphene-based nanoelectronics. Both theoretical physics and potential applications of graphene now require the controllable synthesis of high quality graphene. Epitaxial growth on transition metal surfaces is one of the most effective routes for growing graphene. In recent years, much research effort has been devoted to graphene growth on various metal surfaces, such as Ru(0001),<sup>[9–18]</sup> Ni(111),<sup>[19–23]</sup> Pt(111),<sup>[24,25]</sup> Ir(111),<sup>[26–30]</sup> and Cu.<sup>[31,32]</sup> High quality graphene with controlled dimension and thickness is of considerable importance. In this work, we focus on producing high quality sub-monolayer, monolayer, and bilayer graphene on Ru(0001) surfaces.

## 2. Methods

Our serial experiments were carried out in a UHV Omicron system whose base pressure was lower than  $2 \times 10^{-10}$  mbar. The system is equipped with a room temperature scanning tunneling microscope (RT-STM, Omicron), low energy electron diffraction (LEED) optics, an electron beam heater (EBH), and a gas station that can introduce oxygen or ethylene (purity of 99.995%, Beijing Huayuan Gas Chemical Industry Co., Ltd) into the UHV chamber through a leak valve. Single-crystal Ru(0001), purchased from MaTeck, was sputtered by Ar<sup>+</sup> many times and annealed at 800 °C for 10 min. After which, the single-crystal Ru(0001) was annealed in oxygen at 800 °C to remove the residual carbon and it was then flashed to 1300 °C for 10 s to remove the oxide.<sup>[33]</sup> The clean Ru(0001) surface was checked by LEED and STM. Graphene was then fabricated by the decomposition of ethylene on the as-prepared Ru(0001) surface. Table 1 provides the detailed experimental parameters of producing high quality sub-monolayer, monolayer, and bilayer graphene on the Ru(0001) substrate.

**Table 1.** Parameters for producing high quality sub-monolayer, monolayer, and bilayer graphene on Ru(0001).

Graphene	Temperature of Ru substrate/°C	Pressure of ethylene/10 <sup>-6</sup> mbar	Time of exposure/s	Cooling rate/°C·min <sup>-1</sup>
Sub-monolayer	800	1.3	20	14
Monolayer	800	1.3	100	14
Bilayer	800	1.3	300	5

\*Project supported by the National Basic Research Program of China (Grant Nos. 2013CBA01600 and 2011CB932700) and the National Natural Science Foundation of China (Grant Nos. 61222112 and 11334006).

<sup>†</sup>Corresponding author. E-mail: [xlin@ucas.ac.cn](mailto:xlin@ucas.ac.cn)

<sup>‡</sup>Corresponding author. E-mail: [ylwang@iphy.ac.cn](mailto:ylwang@iphy.ac.cn)

<sup>§</sup>Corresponding author. E-mail: [hjgao@iphy.ac.cn](mailto:hjgao@iphy.ac.cn)

### 3. Results and discussion

Two routes are known for growing graphene islands on a Ru(0001) surface. One is exposing the Ru(0001) surface to ethylene at room temperature and then heating it to 800 °C,<sup>[34]</sup> and the other is exposing the Ru(0001) surface to 20 L ethylene at 800 °C. We carried out both procedures, and found that the latter can prepare high quality graphene islands without defects, as shown in Fig. 1(a). The lateral size of these graphene islands was about 15 nm and they had very straight zigzag edges. Due to the strong interactions between graphene and the Ru substrate, the typical moiré pattern formed in the graphene islands.<sup>[35]</sup> In the atomic resolution STM image (Fig. 1(b)), the inner part of each graphene island is intact without any atomic defects. The LEED pattern (Fig. 1(c)) demonstrates that the graphene is well ordered and aligned with respect to the Ru substrate. However, in the zoomed in LEED pattern image (Fig. 1(d)), the signal of the moiré pattern is not clear, which is attributed to the low coverage of the graphene.

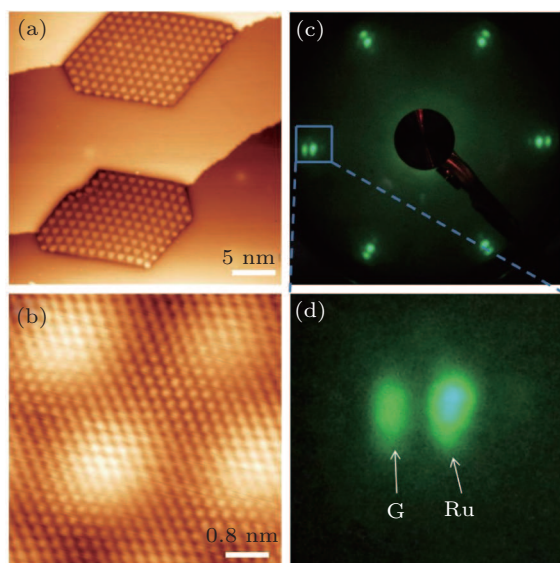


**Fig. 1.** (color online) STM images and LEED patterns of sub-monolayer graphene on Ru(0001). (a) STM image of graphene islands. (b) Atomic resolution STM image of graphene. (c) Corresponding LEED pattern of sub-monolayer graphene shown in panel (a). (d) Zoomed in image of the area enclosed by the blue rectangle in panel (c), showing the LEED signals from graphene and the Ru substrate.

Unlike the graphene islands, the monolayer graphene was grown by exposing clean Ru(0001) to 100 L ethylene at 800 °C.<sup>[17]</sup> Graphene covered all of the terraces and formed a very regular moiré pattern (Fig. 2(a)). In the zoomed in STM image (Figure 2(b)), the graphene seems to be perfect without any defects. From the corresponding LEED patterns (Figs. 2(c) and 2(d)), the signals from graphene and the moiré pattern were observed. By fully investigating the sample surface, we found that monolayer graphene is single-crystalline

and covers the whole Ru(0001) surface. So the size of high quality monolayer graphene depends only on the size of the single-crystal Ru substrate.

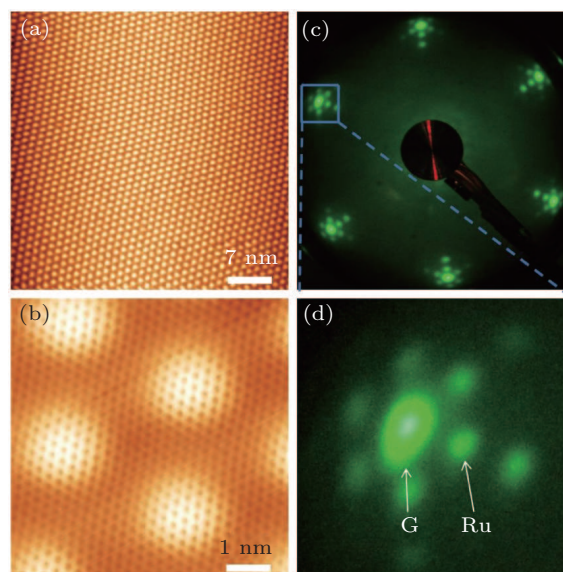


**Fig. 2.** (color online) STM images and LEED patterns of monolayer graphene on Ru(0001). (a) STM image of monolayer graphene. (b) Atomic resolution STM image of monolayer graphene on Ru(0001). (c) Corresponding LEED pattern of monolayer graphene shown in panel (a). (d) Zoomed in image of the area enclosed by the blue rectangle in panel (c), showing the LEED signals from graphene, moiré pattern, and the Ru substrate.

Monolayer graphene on Ru(0001) is n-doped and absent of the properties of free-standing graphene due to the strong coupling between graphene and the Ru(0001) substrate.<sup>[36,37]</sup> However, the growth of bilayer graphene on Ru(0001) is a feasible route to obtain graphene that approximates the intrinsic graphene. By exposing a clean Ru surface to 300 L ethylene at 800 °C, and then cooling it down to room temperature at a rate of 5 °C/min, high quality and large-area bilayer graphene was grown on the Ru(0001) surface. Two kinds of structures were found on the bilayer graphene surface. One is pretty flat graphene with no moiré pattern, as shown in Fig. 3(a). The lateral size of this structure reaches up to 60 nm. Atomic resolution STM images (Fig. 3(b)) show that the graphene is defect-free. The maximum corrugation is about 30 pm, and the apparent height difference between the two carbon sublattices of graphene in the second layer is about 5 pm. According to the previous combined research of angle-resolved photoemission spectroscopy and scanning tunneling microscopy, the second layer has an AA stacking sequence with respect to the first layer.<sup>[38]</sup> In this new study, another structure was found on the bilayer graphene surface, which retains the moiré pattern like the monolayer graphene on Ru(0001) (Fig. 3(c)). The zoomed in STM image (Fig. 3(d)) reveals that the bilayer graphene is intact without any defects, and the corrugation of the bilayer graphene is smaller than that of the monolayer graphene on

Ru(0001). Gradual alternations between AB (Bernal type) and AA stackings are present in this structure.<sup>[39]</sup> By careful large-area scanning, we found that the two structures are present on the surface by turns, which we ascribe to the weak interactions between the second graphene layer and the Ru substrate along with stress relaxation in the second layer of graphene. In our STM results, the areal proportion of the first structure to the second structure is about 4:6. Figures 3(e) and 3(f) show the corresponding LEED patterns of bilayer graphene

on Ru(0001). The LEED patterns have many similarities to that of monolayer graphene on Ru(0001), the only difference is that the signal intensity from the moiré pattern in Fig. 3(f) is much stronger than that of monolayer graphene on Ru(0001). It can be inferred from this that the signal of the moiré pattern in the LEED of the monolayer graphene came from the moiré corrugation in the monolayer, while the LEED signal of the moiré pattern of bilayer graphene came from both the bottom layer and the second structure in the upper layer (Fig. 3(c)).

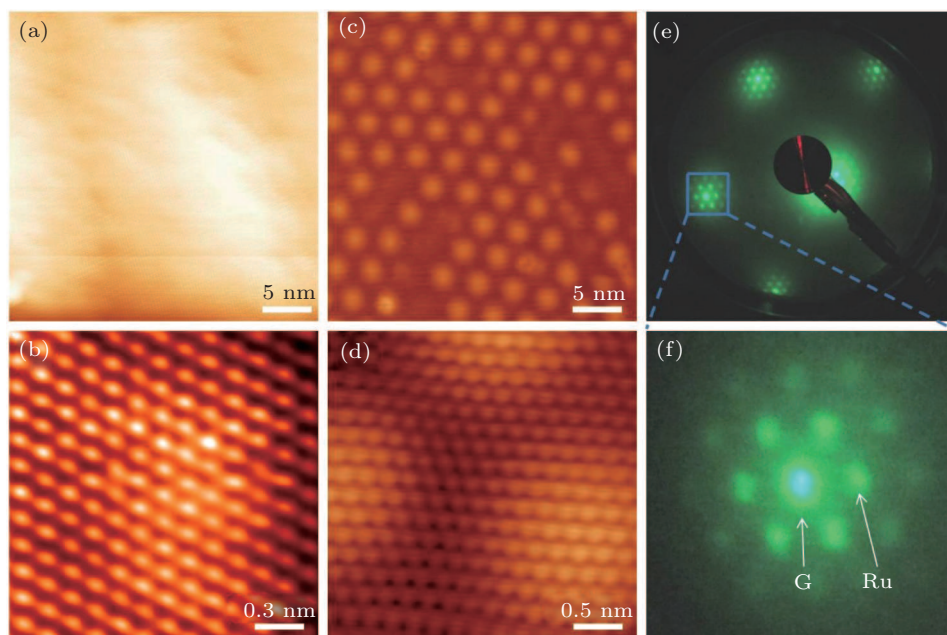


**Fig. 3.** (color online) STM images and LEED patterns of bilayer graphene on Ru(0001). (a) STM image of bilayer graphene without moiré pattern. (b) Atomic resolution STM image of bilayer graphene shown in panel (a). (c) STM image of bilayer graphene with moiré pattern. (d) Atomic resolution STM image of bilayer graphene shown in panel (c). (e) Corresponding LEED pattern of bilayer graphene. (f) Zoomed in image of the area enclosed by the blue rectangle in panel (e), showing the LEED signals from graphene, moiré pattern, and the Ru substrate.

Besides characterization by STM and LEED, Raman spectroscopies of the samples with different graphene coverages were also performed. As shown in Fig. 4, the Raman spectra of graphene islands and monolayer graphene on Ru(0001) are flat lines without the characteristic peaks of graphene. This is attributed to the very strong coupling between graphene and the Ru substrate, which prevents first order scattering, the one-phonon second order double-resonance process, and the two-phonon second order resonance process.<sup>[40,41]</sup> However, the Raman spectroscopy of the bilayer graphene on Ru(0001) contains the D, G, and 2D peaks of graphene. Since the Raman intensity ratio between 2D and G bands is 2:1, the graphene is confirmed as a free-standing monolayer,<sup>[40–43]</sup> which is consistent with the bottom layer of graphene acting as a buffering layer. The bottom layer effectively decouples the interaction between graphene and its Ru(0001) substrate. In addition, the very low intensity of the D band, which mostly comes from the step edge of the sec-

ond layer graphene,<sup>[41]</sup> indicates the high quality of the bilayer graphene.

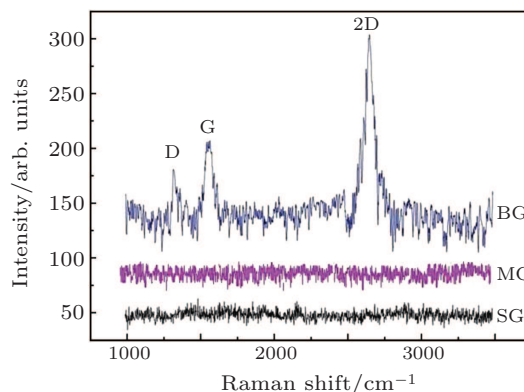


**Fig. 4.** (color online) Raman spectra of sub-monolayer graphene (SG), monolayer graphene (MG), and bilayer (BG) graphene on Ru(0001). Raman spectra of sub-monolayer graphene (black curve) and monolayer graphene (red curve) show no characteristic peaks of graphene. The Raman spectrum of bilayer graphene (blue curve) shows a G peak and a 2D band feature.

## 4. Conclusion

We report the synthesis of high quality sub-monolayer, monolayer, and bilayer graphene on Ru(0001). Exposing a clean Ru(0001) surface to a small dose of ethylene at high substrate temperature of 800 °C leads to the formation of graphene islands on Ru(0001). The size of the graphene islands can be controlled by adjusting the dosage of ethylene. High quality one-monolayer graphene was synthesized with a 100 L dosage of ethylene. By further increasing the dosage of ethylene to 300 L and reducing the cooling rate to 5 °C/min, high quality bilayer graphene was obtained on the Ru(0001) substrate. Raman data revealed that the second (upper) layer behaves more like free-standing graphene. Considering the transferability of the second layer, our method would lead to many applications in both basic research and graphene based nano-electronics.

## References

- [1] Novoselov K S, Geim A. K, Morozov S V, Jiang D, Zhang Y, Dubonos S V, Grigorieva I V and Firsov A A 2004 *Science* **306** 666
- [2] Novoselov K S, Geim A K, Morozov S V, Jiang D, Katsnelson M I, Grigorieva I V, Dubonos S V and Firsov A A 2005 *Nature* **438** 197
- [3] Xu D, Skachko I, Barker A and Andrei E Y 2008 *Nat. Nanotechnol.* **3** 491
- [4] Morozov S V, Novoselov K S, Katsnelson M I, Schedin F, Eilas D C, Jaszczak J A and Geim A K 2008 *Phys. Rev. Lett.* **100** 016602
- [5] Chen J H, Jang C, Xiao S D, Ishigami M and Fuhrer M S 2008 *Nat. Nanotechnol.* **3** 206
- [6] Novoselov K S, Jiang Z, Zhang Y, Morozov S V, Stormer H L, Zeitler U, Maan J C, Boebinger G S, Kim P and Geim A K 2007 *Science* **315** 1379
- [7] Zhang Y, Tan Y W, Stormer H L and Kim P 2005 *Nature* **438** 201
- [8] Novoselov K S, Geim A K, Morozov S V, Jiang D, Katsnelson M I, Grigorieva I V, Dubonos S V and Firsov A A 2005 *Nature* **438** 197
- [9] Marchini S, Gunther S and Wintterlin J 2007 *Phys. Rev. B* **76** 075429
- [10] Pan Y, Shi D X and Gao H J 2007 *Chin. Phys.* **16** 3151
- [11] Loginova E, Bartelt N C, Feibelman P J and McCarty K F 2008 *New J. Phys.* **10** 093026.
- [12] Sutter P W, Flege J I and Sutter E A 2008 *Nat. Mater.* **7** 406
- [13] de Parga A L V, Calleja F, Borca B, Passeggi M C G, Hinarejos J J, Guinea F and Miranda R 2008 *Phys. Rev. Lett.* **100** 056807
- [14] Sutter E, Acharya D P, Sadowski J T and Sutter P 2009 *Appl. Phys. Lett.* **94** 133101
- [15] McCarty K F, Feibelman P J, Loginova E and Bartelt N C 2009 *Carbon* **47** 1806
- [16] Borca B, Calleja F, Hinarejos J J, de Parga A L V and Miranda R J J 2009 *J. Phys.: Condens. Matter* **21** 134002
- [17] Pan Y, Zhang H G, Shi D X, Sun J T, Du S X, Liu F and Gao H J 2009 *Adv. Mater.* **21** 2777
- [18] Zhang H, Fu Q, Cui Y, Tan D and Bao X 2009 *J. Phys. Chem. C* **113** 8296
- [19] Farias D, Shikin A M, Rieder K H and Dedkov Y S J 1999 *J. Phys.: Condens. Matter* **11** 8453
- [20] Shikin A M, Prudnikova G V, Adamchuk V K, Moresco F and Rieder K H 2000 *Phys. Rev. B* **62** 13202
- [21] Starodubov A G, Medvetkii M A, Shikin A M and Adamchuk V K 2004 *Phys. Solid State* **46** 1340
- [22] Dedkov Y S, Fonin M, Rudiger U and Laubschat C 2008 *Appl. Phys. Lett.* **93** 022509
- [23] Varykhalov A, Sanchez-Barriga J, Shikin A M, Biswas C, Vescovo E, Rybkin A, Marchenko D and Rader O 2008 *Phys. Rev. Lett.* **101** 157601
- [24] Ueta H, Saida M, Nakai C, Yamada Y, Sasaki M and Yamamoto S 2004 *Surf. Sci.* **560** 183
- [25] Starr D E, Pazhetnov E M, Stadnichenko A I, Boronin A I and Shaikhutdinov S K 2006 *Surf. Sci.* **600** 2688
- [26] Klusek Z, Kozłowski W, Waqar Z, Datta S, Burnell-Gray J S, Makarenko I. V, Gall N R, Rutkov E V, Tontegode A Y and Titkov A N 2005 *Appl. Surf. Sci.* **252** 1221
- [27] N'Diaye A T, Bleikamp S, Feibelman P J and Michely T 2006 *Phys. Rev. Lett.* **97** 215501
- [28] N'Diaye A T, Coraux J, Plasa T N, Busse C and Michely T 2008 *New J. Phys.* **10** 043033
- [29] Coraux J, N'Diaye A T, Busse C and Michely T 2008 *Nano Lett.* **8** 565
- [30] Coraux J, N'Diaye A T, Engler M, Busse C, Wall D, Buckanie N, Heringdorf F J M Z, van Gastei R, Poelsema B and Michely T 2009 *New J. Phys.* **11** 023006
- [31] Wang W R, Liang C, Li T, Yang H, Lu N and Wang Y L 2013 *Chin. Phys. Lett.* **30** 028102
- [32] Feng D J, Huang W Y, Jiang S Z, Ji W and Jia D F 2013 *Acta Phys. Sin.* **62** 054202 (in Chinese)
- [33] Mao J H, Huang L, Pan Y, Gao M, He J F, Zhou H T, Guo H M, Tian Y, Zou Q, Zhang L Z, Zhang H G, Wang Y L, Du S X, Zhou X J, Castro Neto A H and Gao H J 2012 *Appl. Phys. Lett.* **100** 093101
- [34] Huang L, Xu W Y, Que Y D, Pan Y, Gao M, Pan L D, Guo H M, Wang Y L, Du S X and Gao H J 2012 *Chin. Phys. B* **21** 088102
- [35] Wintterlin J and Bocquet M L 2009 *Surf. Sci.* **603** 1841
- [36] Martoccia D, Willmott P R, Brugger T, Bjorck M, Gunther S, Schlepütz C M, Cervellino A, Pauli S A, Patterson B D, Marchini S, Wintterlin J, Moritz W and Greber T 2008 *Phys. Rev. Lett.* **101** 126102
- [37] Moritz W, Wang B, Bocquet M L, Brugger T, Greber T, Wintterlin J and Gunther S 2010 *Phys. Rev. Lett.* **104** 136102
- [38] Papagno M, Pacile' D, Topwal D, Moras P, Sheverdyayeva P M, Natterer F D, Lehnert A, Rusponi S, Dubout Q, Calleja F, Frantzeskakis E, Pons S, Fujii J, Vobornik I, Grioni M, Carbone C and Brune H 2012 *ACS Nano* **6** 9299
- [39] Que Y D, Xiao W D, Fei X M, Chen H, Huang L, Du S X and Gao H J 2014 *Appl. Phys. Lett.* **104** 093110
- [40] Ferrari A C, Meyer J C, Scardaci V, Casiraghi C, Lazzeri M, Mauri F, Piscanec S, Jiang D, Novoselov K S, Roth S and Geim A K 2006 *Phys. Rev. Lett.* **97** 187401
- [41] Malard L M, Pimenta M A, Dresselhaus G and Dresselhaus M S 2009 *Phys. Rep.* **473** 51
- [42] Reina A, Jia X T, Ho J, Nezich D, Son H B, Bulovic V, Dresselhaus M S and Kong J 2009 *Nano Lett.* **9** 30
- [43] Wang Y, Ni Z, Yu T, Shen Z X, Wang H, Wu Y, Chen W and Wee A T S 2008 *J. Phys. Chem.* **100** 10637